

# SCIENTIFIC REPORTS



OPEN

## Dapagliflozin rescues endoplasmic reticulum stress-mediated cell death

Ryo Shibusawa<sup>1</sup>, Eijiro Yamada<sup>1</sup>, Shuichi Okada<sup>1</sup>, Yasuyo Nakajima<sup>1</sup>, Claire C. Bastie<sup>2</sup>, Akito Maeshima<sup>3</sup>, Kyoichi Kaira<sup>4</sup> & Masanobu Yamada<sup>1</sup>

The new type 2 diabetes drug, dapagliflozin, reduces blood glucose levels and body weight by inhibiting sodium glucose transporter 2 (SGLT2) in proximal tubular cells. SGLT2 inhibitors might modulate glucose influx into renal tubular cells, thereby regulating the metabolic conditions that cause endoplasmic reticulum (ER) stress in the cells. In this study, we examined the effect of dapagliflozin on ER stress in the HK-2 proximal tubular cell line and in the kidney of db/db mice to characterise its function in diabetic nephropathy (DN). We found that dapagliflozin regulated ER stress-mediated apoptosis *in vitro* and *in vivo*. Only the eIF2 $\alpha$ -ATF4-CHOP pathway was regulated under these conditions. Notably, the drug rescued C2 ceramide-induced ER stress-mediated apoptosis and ER stress-mediated apoptosis, which might occur in DN, in db/db mice. Our study shows a novel role for dapagliflozin as an inhibitor of ER stress and suggests that dapagliflozin might be useful for the prevention of DN.

The number of patients with diabetes has increased globally, partly due to changes in dietary habits and a lack of exercise<sup>1-3</sup>. Diabetes leads to an array of additional complications, and the disease and its prevention have become a worldwide priority<sup>4</sup>. One of the major complications of diabetes is diabetic nephropathy (DN), which is the leading cause of end-stage renal disease<sup>5,6</sup>. Several studies have shown that the diabetic kidney is exposed to various environmental stressors that may cause endoplasmic reticulum (ER) stress<sup>5,6</sup>.

The ER is the major site for protein folding<sup>7,8</sup>. When protein loading exceeds its capacity, unfolded protein response (UPR) is activated to suppress protein synthesis and increase both the ER folding capacity and misfolded protein degradation, resulting in the restoration of cellular homeostasis<sup>7</sup>. If the stress response is prolonged or beyond ER folding capacity, it may lead to cell death<sup>7</sup>. UPR is mediated by three canonical pathways: RNA-dependent protein kinase-like ER kinase (PERK), activating transcription factor 6 (ATF6), and inositol-requiring enzyme 1 (IRE1) pathways<sup>7</sup>. PERK is present in the ER and its phosphorylation at Ser51 of eukaryotic translation initiation factor 2 $\alpha$  (eIF2 $\alpha$ ) inhibits protein translation<sup>7,9</sup>. Notably, ATF6 activated by phosphorylation of eIF2 $\alpha$  initiates the transcription of CCAAT/enhancer-binding protein-homologous protein (Chop/Gadd153), which is critical in ER stress-induced apoptosis<sup>7,9,10</sup>. Although ATF6 also exists in the ER, it is transported to the Golgi apparatus under stress conditions and cleaved by site-1 and site-2 proteases<sup>7,11</sup>. Cleaved ATF6 enters the nucleus and transcribes adaptive chaperons such as Bip/GRP78<sup>7,11</sup>. IRE1 exerts endoribonuclease and kinase activities<sup>7,12</sup>. The endoribonuclease activity of IRE1 cleaves the X-box binding protein 1 (XBP1) to generate spliced XBP1 (XBP1s), a transcription factor involved in the survival response<sup>7,12</sup>. It has been shown that the IRE1 $\alpha$ -XBP1 pathway plays a role in insulin resistance by activating JNK and suppressing insulin signalling; however, the relationship between ER stress and diabetic complications is still largely unknown<sup>13-15</sup>.

Ceramides are important molecules involved in sphingolipid metabolism and play critical roles in the regulation of various cellular functions, including cell proliferation, differentiation, migration, and apoptosis<sup>16,17</sup>. The short side chain C2 ceramide easily invades cells, exerts physiological activity, and enhances caspase-dependent apoptosis<sup>17</sup>. It has been shown that plasma C2 ceramide levels also increase in diabetes<sup>18</sup>. They play an important

<sup>1</sup>Department of Medicine and Molecular Science, Gunma University Graduate School of Medicine, Maebashi, 371-8511, Japan. <sup>2</sup>Division of Biomedical Sciences, Warwick Medical School, Coventry, West Midlands, United Kingdom.

<sup>3</sup>Division of Nephrology, Department of Internal Medicine, Jichi Medical University, Shimotsuke, Tochigi, Japan.

<sup>4</sup>Department of Oncology Clinical Development, Gunma University Graduate School of Medicine, Maebashi, 371-8511, Japan. Correspondence and requests for materials should be addressed to E.Y. (email: [eijiro.yamada@gunma-u.ac.jp](mailto:eijiro.yamada@gunma-u.ac.jp))

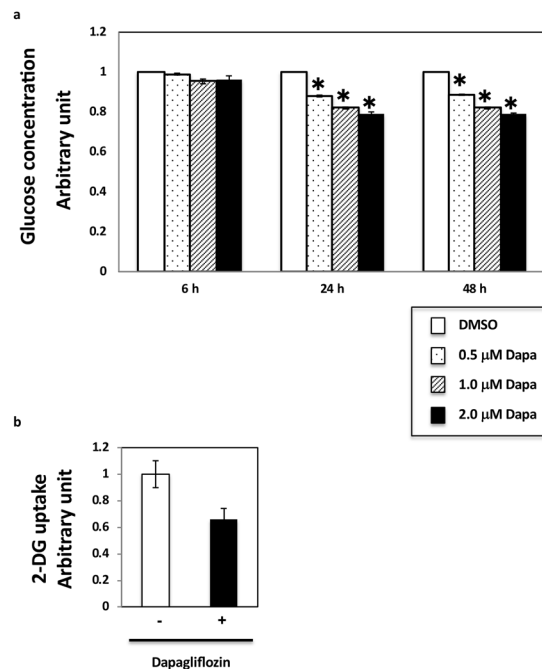


**Figure 1.** Dapagliflozin regulates glucose influx into HK-2 renal proximal tubular epithelial cells. **(a)** HK2 cells were incubated with the indicated dapagliflozin concentration for the indicated times and were collected for glucose analysis. Glucose concentration in HK2 cells was assessed using the PicoProbe Glucose Fluorometric Assay Kit (BioVision).  $P < 0.05$  ( $n = 3-5$ ). **(b)** Glucose influx in HK2 cells incubated with 2  $\mu\text{M}$  dapagliflozin for 36 h was measured using the 2-Deoxyglucose Uptake Measurement Kit (COSMO BIO Co. Ltd., Tokyo Japan) according to the manufacturer's instructions.

pathophysiological role not only in the development of diabetes itself but also in diabetic complications<sup>19-22</sup>. C2 ceramide induces apoptosis by multiple mechanisms, namely activation of the extrinsic apoptotic pathway, increasing cytochrome c release, generation of free radicals, and induction of ER stress<sup>19,20</sup>.

Glomerular damage is considered the main characteristic in the kidneys of patients with DN. However, it was recently suggested that alterations in the renal tubule might also contribute to the pathogenesis of DN<sup>23</sup>. Notably, the novel type 2 diabetes drug dapagliflozin reduces blood glucose and body weight by inhibiting sodium glucose transporter 2 (SGLT2) in the proximal tubular cells<sup>24</sup>. We hypothesised that modulation of SGLT2 activity might affect glucose influx into renal tubular cells. Inhibiting SGLT2 with dapagliflozin may regulate the metabolic conditions that cause ER stress in these cells<sup>25</sup>. Therefore, in this study, we examined the effect of the SGLT2 inhibitor dapagliflozin on UPR in both the *in vitro* proximal tubular cell line HK-2 and *in vivo*.

## Results

**Dapagliflozin mediates glucose influx and ER stress in HK2 cells.** Dapagliflozin inhibits SGLT2-mediated renal glucose reabsorption in renal proximal tubular epithelial cells, thereby lowering the plasma blood glucose levels in patients with diabetes<sup>10,12,13</sup>. To identify additional functions of SGLT2, we used HK2 cells, an *in vitro* cell model of renal proximal tubular epithelial cells. First, we performed a series of dose-response and time course experiments to determine the effects of dapagliflozin on glucose levels in HK2 cells. Since a maximum plasma concentration ( $C_{\text{max}}$ ) of dapagliflozin of approximately 0.5  $\mu\text{M}$  and 0.2–20  $\mu\text{M}$  was used in previous studies, we initially choose 0.5–2.0  $\mu\text{M}$  dapagliflozin. We found that intracellular glucose concentrations in cells treated with 2  $\mu\text{M}$  dapagliflozin for 24–48 h decreased by 20%, compared to those in control (non-treated) cells (Fig. 1a). Since the effect of dapagliflozin was maximum at this condition, we decided to use it for all *in vitro* experiments. Notably, glucose influx measured with tracers decreased by around 40% under this condition (Fig. 1b). As glucose influx could potentially mediate ER stress in cells and tissues, we next examined the markers of ER stress in dapagliflozin-treated HK-2 cells. We first evaluated the basal level of ER stress. Since the basal level of ER stress might depend on cell confluency, we plated different cell numbers on 24 wells and found that the phosphorylation of eIF2 $\alpha$ , a marker for ER stress, was the maximum 48 h after we plated  $1 \times 10^6$  cells in 24 wells (Supplementary Fig. 1). Under these conditions, dapagliflozin decreased the phosphorylation of eIF2 $\alpha$  (Fig. 2a,b). To confirm this, we examined the downstream targets of eIF2 $\alpha$ . As shown in Fig. 2c, the decrease in ATF4 expression levels in dapagliflozin-treated HK2 cells was parallel to the decrease in eIF2 $\alpha$  phosphorylation levels. In contrast, dapagliflozin had no effect on total and cleaved forms of ATF6 (Fig. 2d,e) or phosphorylation of IRE1 $\alpha$  (Fig. 2d,f), indicating that it mediated ER stress only through the eIF2 $\alpha$  pathway.

CHOP has recently been reported as a downstream target of eIF2 $\alpha$  and has been described as a marker of ER-mediated apoptosis<sup>7,9,10</sup>. As shown in Fig. 2g, CHOP expression levels also decreased in dapagliflozin-treated HK2 cells. Because CHOP expression levels decreased, we next examined caspase-3 activity to determine

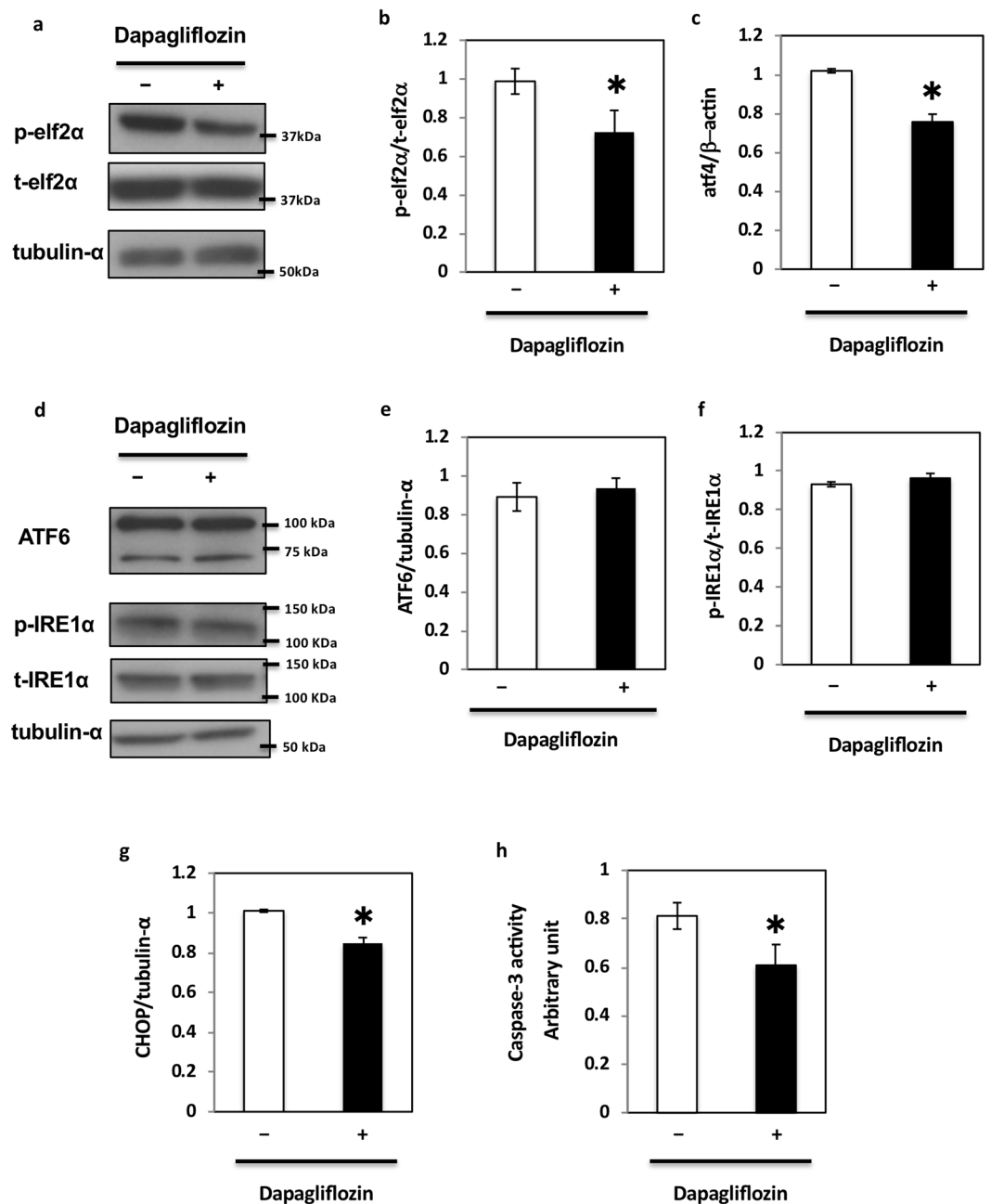


**Figure 2.** Dapagliflozin regulates unfolded protein response in HK-2 cells. (a) HK2 cells were incubated with 2  $\mu$ M dapagliflozin for 36 h and collected for protein expression analysis. These immunoblots are representative of  $n = 5$  experiments performed independently. (b) Signal quantification of the expression levels for  $S^{51}$  phosphorylation of eIF2 $\alpha$  normalised with total eIF2 $\alpha$  levels. (c) HK2 cells were incubated with 2  $\mu$ M dapagliflozin for 36 h, and the ATF4 mRNA expression levels were determined by qRT-PCR ( $n = 5$  independent experiments). (d) HK2 cells were incubated with 2  $\mu$ M dapagliflozin for 36 h, collected for protein analysis, and immunoblotted for the indicated proteins. These are representative immunoblots independently performed five times. (e,f) Signal quantification of the expression levels of ATF6 normalised with tubulin- $\alpha$  (e) and the expression levels for  $S^{724}$  phosphorylation of IRE1 $\alpha$  normalised with total IRE1 $\alpha$  levels (f). (g) HK2 cells were incubated with 2  $\mu$ M dapagliflozin for 36 h, and the expression level of CHOP mRNA was determined by qRT-PCR ( $n = 5$  independent experiments). (h) HK2 cells were incubated with 2  $\mu$ M dapagliflozin for 36 h and caspase-3 activity levels were measured using a caspase-3 fluorescence assay kit (MBL) ( $n = 5$  independent experiments).

the apoptotic status of these cells. As shown in Fig. 2h, we observed a 20% reduction in caspase-3 activity in dapagliflozin-treated cells. This paralleled the reduction in glucose influx, phosphorylation of eIF2 $\alpha$ , and expression of CHOP, suggesting that dapagliflozin might regulate apoptosis through the eIF2 $\alpha$ -CHOP axis in HK2 cells.

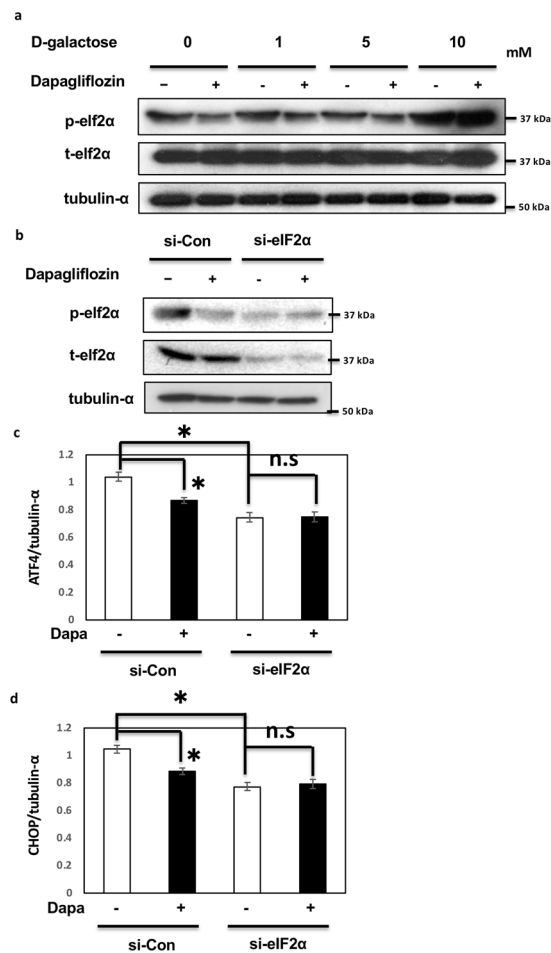


**Figure 3.** Dapagliflozin regulates unfolded protein response through the eIF2 $\alpha$  pathway in HK-2 cells. **(a)** HK2 cells were treated with 2  $\mu$ M dapagliflozin for 36 h with varying concentrations of D-galactose. Immunoblotting was performed with the indicated antibodies. **(b)** HK2 cells were transfected by siRNA for eIF2 $\alpha$  and incubated with 2  $\mu$ M dapagliflozin for 36 h. Immunoblotting was performed with the indicated antibodies. **(c,d)** HK2 cells were transfected by siRNA for eIF2 $\alpha$  and incubated with 2  $\mu$ M dapagliflozin for 36 h. The mRNA expression levels of ATF4 and CHOP were determined by qRT-PCR (n = 5 independent experiments).

**The eIF2 $\alpha$  pathway is critical for the effects of dapagliflozin on ER stress in HK2 cells.** To examine whether the effects of dapagliflozin were the result of reduced glucose uptake or a direct effect of dapagliflozin, the medium of HK-2 cells was supplemented with different concentrations (0–10 mM) of D-galactose before the analyses of eIF2 $\alpha$  and CHOP expression. As shown in Fig. 3a, dapagliflozin reduced the phosphorylation of eIF2 $\alpha$ , except in the presence of 10 mM D-galactose, indicating that the effect of dapagliflozin was due to reduced glucose uptake. To investigate whether the eIF2 $\alpha$  pathway is critical for the effect of dapagliflozin on ER stress, siRNA-mediated knockdown of eIF2 $\alpha$  was performed, and ATF4 and CHOP expression was determined. As shown in Fig. 3c,d, siRNA-mediated knockdown of eIF2 $\alpha$  reduced the basal levels of ATF4 and CHOP. Notably, the effects of dapagliflozin on ATF4 and CHOP were completely abolished under these conditions, indicating that the eIF2 $\alpha$  pathway plays a crucial role in mediating the effects of dapagliflozin (Fig. 3c,d).

#### Dapagliflozin rescued C2 ceramide-induced ER stress through the eIF2 $\alpha$ -CHOP pathway.

Our data suggested that dapagliflozin mediated apoptosis through ER stress; however, whether dapagliflozin could be a key factor in the prevention of diabetic kidney disease remained to be determined. Therefore, to confirm the effect of dapagliflozin on ER stress and to examine its effect on the kidney in metabolic diseases, we used C2 ceramide, which not only induces ER stress but also acts as a pathogen in metabolic diseases<sup>19–22</sup>. As shown in Fig. 4, dapagliflozin had no effect on GLUT2 and SGLT2 expression (Fig. 4a–c) but decreased eIF2 $\alpha$  phosphorylation (Fig. 4a,d) and ATF4 expression (Fig. 4e). C2 ceramide enhanced eIF2 $\alpha$  phosphorylation (Fig. 4a,d) and ATF4 expression (Fig. 4e). Dapagliflozin partially reduced these effects, suggesting that it might alleviate C2 ceramide-induced ER stress. Notably, C2 ceramide-induced CHOP expression and caspase-3 activity were also inhibited by dapagliflozin (Fig. 5a,b). C2 ceramide reduced cell number and protein amounts in HK-2 cells, indicating cell death. However, dapagliflozin rescued the effect of C2 ceramide (Fig. 5c,d) by

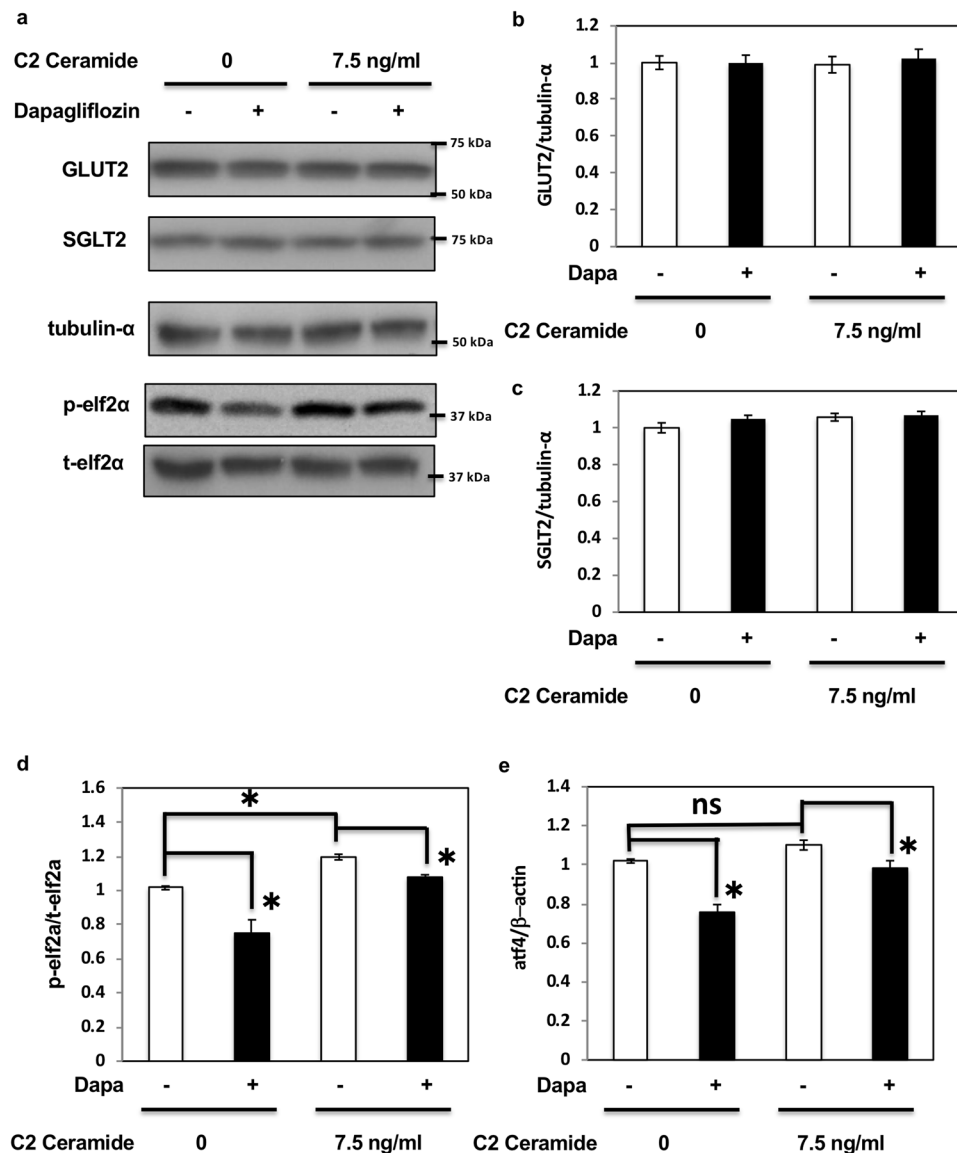


**Figure 4.** Dapagliflozin rescued C2 ceramide-induced ER stress in HK2 cells. (a) HK2 cells were treated with 2  $\mu$ M dapagliflozin for 36 h with or without 7.5 ng/mL C2 ceramide, and immunoblotting was performed with the indicated antibodies (b,c). Signal quantification of the expression levels of GLUT2 (b) and SGLT2 (c) normalised with tubulin- $\alpha$  levels. (d) Signal quantification of the expression levels of S<sup>51</sup> phosphorylation of elf2 $\alpha$  normalised with total elf2 $\alpha$  levels. (e) HK2 cells were incubated with 2  $\mu$ M dapagliflozin for 36 h, and the mRNA expression levels of ATF4 were determined by qRT-PCR (n = 5 independent experiments).

regulating apoptosis and necrosis (Fig. 5e,f). These data indicate that dapagliflozin might attenuate the metabolic state that induces renal cell death and exhibit beneficial effects in preventing DN, independently of blood glucose reduction.

**Dapagliflozin ameliorates ER stress in the kidney of db/db mice *in vivo*.** Our data suggested that dapagliflozin ameliorated glucose-mediated ER stress and apoptosis in HK2 cells, the model of renal proximal tubular epithelial cells *in vitro*. To further examine the effects of dapagliflozin, we repeated these experiments using kidneys of db/db mice, a mouse model of type 2 diabetes<sup>26,27</sup>. Previous reports have shown that ER stress is upregulated in the kidney of db/db mice<sup>28,29</sup>. To explore the effects of dapagliflozin on ER stress in the kidney of db/db mice, the drug was administered orally to the animals every day for 1 week. Similarly to previous studies<sup>30,31</sup>, we did not observe any significant decrease in body weight after only 1 week of treatment (Fig. 6a). However, blood glucose levels significantly decreased with no significant change in the expression level of SGLT2 (Fig. 6b,c). Notably, in these conditions, dapagliflozin decreased elf2 $\alpha$  phosphorylation (Fig. 6d,e) and ATF4 expression independently of body weight change (Fig. 6f). In contrast, dapagliflozin had no effect on total and cleaved forms of ATF6 (Fig. 6g,h) or phosphorylation of IRE1 $\alpha$  (Fig. 6g,i). ATF4 and CHOP expression and

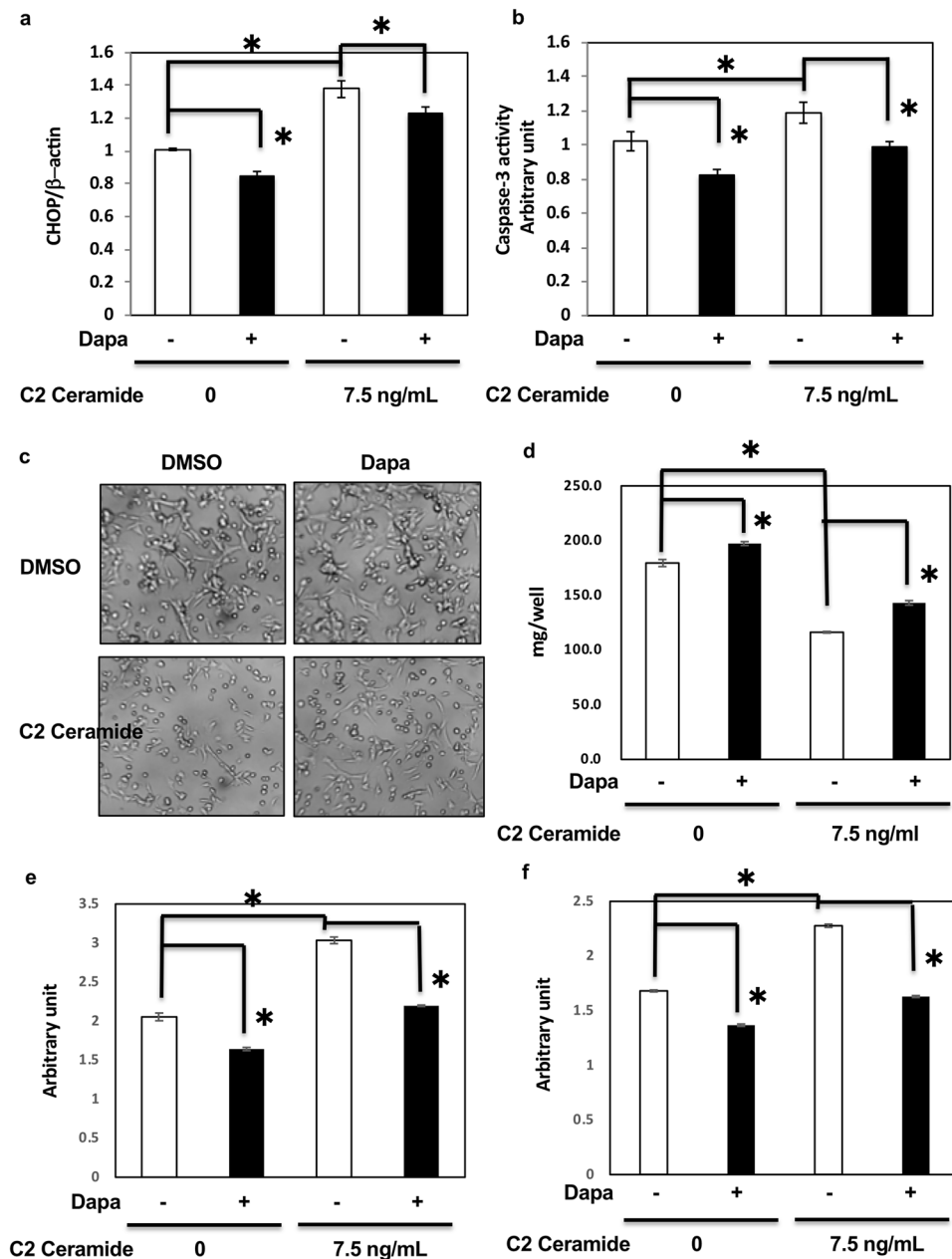


**Figure 5.** Dapagliflozin rescued C2 ceramide-induced cell death in HK2 cells. **(a)** HK2 cells were incubated with 2  $\mu$ M dapagliflozin for 36 h with or without 7.5 ng/ml C2 ceramide, and the expression levels of CHOP mRNA were determined by qRT-PCR (n = 5 independent experiments). **(b)** HK2 cells were treated with 2  $\mu$ M dapagliflozin for 36 h with or without 7.5 ng/ml C2 ceramide, and caspase-3 activity levels were determined (n = 5 independent experiments). **(c,d)** HK2 cells were treated with 2  $\mu$ M dapagliflozin for 48 h with or without 7.5 ng/ml C2 ceramide, and the cells were subjected to microscopic observation **(c)** and protein assay **(d)**. These are representative images from experiments independently performed five times. **(e), (f)** HK2 cells were treated with 2  $\mu$ M dapagliflozin for 48 h with or without 7.5 ng/ml C2 ceramide, and apoptosis and necrosis assay was performed using a Cell Death Detection ELISAplus (Roche, Indianapolis, IN).

caspase-3 activity were also inhibited by dapagliflozin (Fig. 7a–c). These data indicate that dapagliflozin ameliorates ER stress in the kidney of db/db mice *in vivo* and has beneficial effects in preventing DN.

## Discussion

SGLT2 inhibitors are novel type 2 diabetes drugs that reduce blood glucose by inhibiting SGLT2 in the proximal tubules<sup>24,25,32</sup>. Dapagliflozin is an SGLT2 inhibitor that is rapidly absorbed after oral administration. Its maximum plasma concentration (C<sub>max</sub>) is approximately 0.5  $\mu$ M. The working concentration of dapagliflozin has been reported to be 0.1–20  $\mu$ M in HK-2 cells<sup>33–37</sup>. In this study, we treated HK-2 cells with 2  $\mu$ M dapagliflozin based on the findings reported in previous studies.

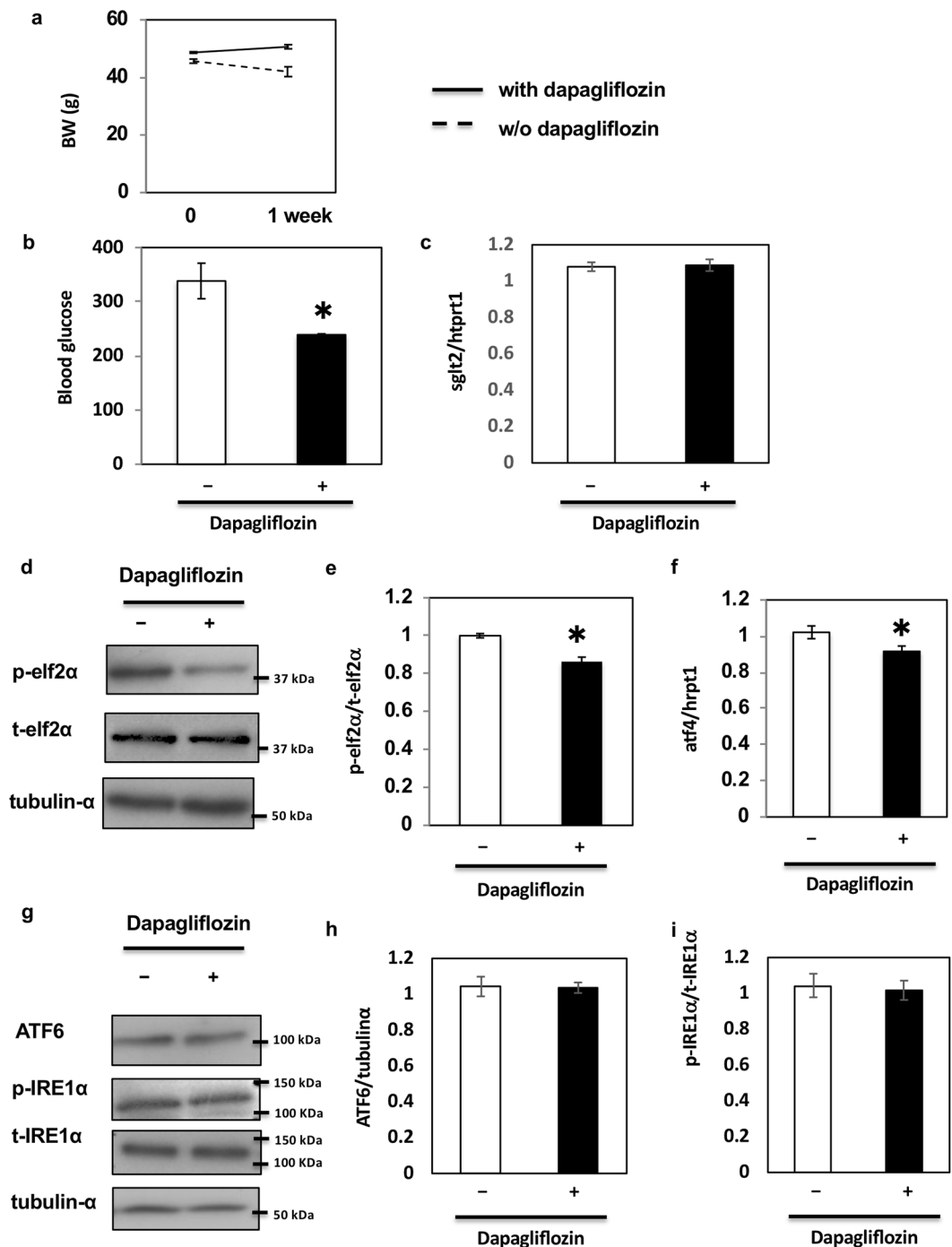


**Figure 6.** Effect of dapagliflozin on ER stress-induced cell death *in vivo*. **(a)** Body weights of db/db mice administered oral dapagliflozin every day for 1 week. **(b)** Blood glucose levels of db/db mice administered dapagliflozin. **(c)** SGLT2 mRNA levels in the kidney of db/db mice were determined by qRT-PCR ( $n = 5$  independent experiments). **(d,g)** The kidneys of db/db mice were utilised for protein expression analysis. These immunoblots are representative of  $n = 5$  experiments performed independently. **(e)** Signal quantification of the expression levels of S<sup>51</sup> phosphorylation of elf2 $\alpha$  normalised with total elf2 $\alpha$ . **(f)** Expression levels of ATF4 mRNAs were determined by qRT-PCR ( $n = 5$  independent experiments). **(h,i)** Signal quantification of the expression levels of ATF6 normalised with tubulin- $\alpha$  **(h)** and the expression levels of S<sup>724</sup> phosphorylation of IRE1 $\alpha$  normalised with total IRE1 $\alpha$  **(i)**.

Changes in glucose influx into the cells might contribute to the metabolic conditions that enhance ER stress in DN. Therefore, we hypothesised that inhibiting SGLT2 might reduce ER stress and protect against proximal tubular cell death. It has been reported that increasing glucose influx into cells might induce but also decrease ER

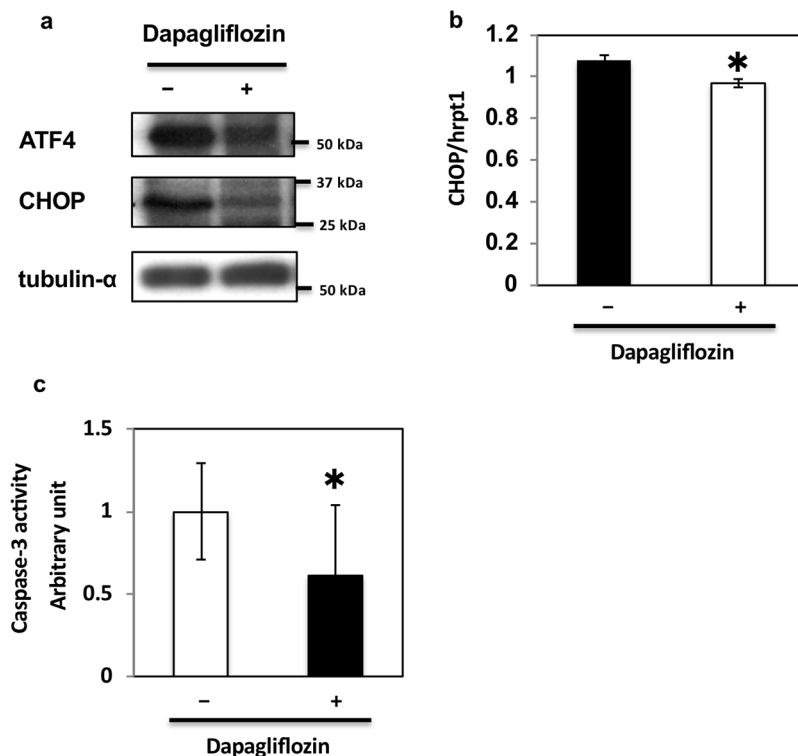


**Figure 7.** Effect of dapagliflozin on ER stress-mediated cell death *in vivo*. (a) The kidneys of db/db mice administered dapagliflozin were immunoblotted with indicated antibodies. (b) CHOP mRNA levels in the kidney of db/db mice administered dapagliflozin were determined by qRT-PCR (n = 5 independent experiments). (c) Caspase-3 activity levels in the kidneys of db/db mice administered dapagliflozin were determined (n = 5 independent experiments).

stress<sup>38–40</sup>. In this study, we demonstrated that dapagliflozin regulates ER stress by reducing glucose concentration as well as glucose influx into HK-2 cells and that it suppresses apoptosis via regulation of the eIF2 $\alpha$ -ATF4-CHOP pathway. The fact that glucose depletion does not induce ER stress but instead ameliorates it in renal cells may appear counter-intuitive. However, several reports have indicated that renal tubular cells are easily subjected to oxidative stress and ER stress-mediated cell death. As high glucose potentially upregulates oxidative stress, this might be one plausible mechanism by which glucose depletion ameliorates ER stress in renal tubular cells<sup>41–43</sup>. Knockdown of eIF2 $\alpha$  counteracted the effect of dapagliflozin. It was shown that the anaesthetic drug propofol inhibits PERK-eIF2 $\alpha$ -ATF4-CHOP activation under ER stress, caspase-3 activation, and apoptosis, whereas it activates the IRE1-XBP1 and ATF6 pathways<sup>44</sup>. These data indicate that the regulation of ER stress is largely dependent on the stimulus itself and pathways regulating ER stress and apoptosis vary with the nature of cells and/or pathology. Our study suggests that the eIF2 $\alpha$ -ATF4-CHOP pathway regulates ER stress in HK2 proximal tubular cells and in the kidney of db/db mice.

ER stress has been associated with many diseases including neurodegenerative disorders, type 2 diabetes, atherosclerosis, or cancer<sup>45</sup>. CHOP is a key protein playing a role in ER stress-induced apoptosis and one of the transcription factors regulated by both PERK-eIF2 $\alpha$ -ATF4 and ATF6<sup>46</sup>. IRE1 $\alpha$  also induces apoptosis through caspases and ASK1-JNK. A positive correlation was observed between the enhanced CHOP expression and cell apoptosis in tubule epithelial cells<sup>47</sup>. Activation of PERK may be a key event in the regulation of CHOP expression<sup>48</sup>. Our findings were consistent with these data and indicated that dapagliflozin might regulate ER stress-induced apoptosis through the PERK-CHOP axis.

Ceramides are generated either by the hydrolysis of sphingomyelin catalysed by sphingomyelinase or by *de novo* synthesis in response to diverse stimuli. Under apoptotic stimuli, ceramides are generated by *de novo* synthesis and promote activation of caspases<sup>49,50</sup>. Notably, ceramides are induced in renal proximal tubular cells in response to hydrogen peroxide or hypoxia/reperfusion<sup>51,52</sup>. When ceramide generation was inhibited using SPT inhibitors and ceramide synthase inhibitors, a reduction in tubular epithelial cell death was observed<sup>22</sup>. Many studies on lipid metabolism in DN have been reported recently<sup>36</sup>. For example, AdipoRon, a therapeutic agent against DN, ameliorates renal ceramide-induced lipotoxicity in type 2 diabetes mellitus<sup>21</sup>. Additionally, investigating the role of ceramide is one of the major fields of study in DN, and researchers have reported excessive ceramide formation in the pathobiological condition of DN<sup>19–22</sup>. Therefore, we examined the effects of dapagliflozin on ER stress and apoptosis after C2 ceramide treatment and demonstrated that dapagliflozin alleviated renal cell death induced by metabolic conditions (i.e. increased glucose influx).

Recent evidence suggested that SGLT2 inhibitors not only have glucose-lowering effects but might also inhibit the progression of DN<sup>33,54</sup>. For example, empagliflozin, the first antidiabetic medication approved for reducing

the risk of cardiovascular death in patients with type 2 diabetes, also reduces the effects of DN<sup>54,55</sup>. Nonetheless, further studies are necessary to investigate the specificity of dapagliflozin for reducing the effects of DN. Future studies should examine whether other SGLT2 inhibitors have potentially beneficial effects on DN as well and determine whether inhibitors of other members of the SGLT family might have similar effects on DN.

In summary, we demonstrated that dapagliflozin lowered glucose influx *in vitro* and regulated ER stress-mediated apoptosis via regulation of eIF2 $\alpha$ -ATF4-CHOP pathway. C2 ceramide treatment on HK-2 cells initiated apoptosis and lipid metabolism disorder in DN. Dapagliflozin partially reduced C2 ceramide-induced ER stress-mediated apoptosis, which might occur in DN. In addition, dapagliflozin ameliorated ER stress in the kidney of db/db mice *in vivo*. These data suggest that dapagliflozin can be used for the prevention of DN itself.

## Materials and Methods

**Antibodies and reagents.** Dapagliflozin and C2 ceramide were purchased from Cayman Chemical (Ann Arbor, MI, USA) and SIGMA-ALDRICH (St. Louis, MO, USA) respectively. Rabbit polyclonal anti-eIF2 $\alpha$ , anti-phospho-eIF2 $\alpha$  Ser51, and anti-ATF4, and mouse monoclonal antibodies were from Cell Signaling Technology Inc. (Boston, MA, USA). Rabbit polyclonal anti-IRE1 $\alpha$  and anti-phospho-IRE1 $\alpha$ , and mouse monoclonal anti-ATF6 antibodies were from Novus Biologicals (Littleton, CO, USA). Mouse monoclonal anti-GAPDH antibody was from MBL (Woods Hole, MA, USA). All other reagents were purchased from Sigma-Aldrich.

**Culture and drug treatment *in vitro*.** The human renal proximal tubular epithelial cell line HK-2 was obtained from ATCC (Manassas, VA, USA). The cells were cultured in a 100-cm<sup>2</sup> dish and grown at 37°C in an atmosphere of 5% CO<sub>2</sub> in air in Keratinocyte-SFM medium supplemented with bovine pituitary extract (0.05 mg/mL) and epithelial growth factor (5 ng/mL; Gibco, Carlsbad, CA, USA). The glucose concentration of the keratinocyte-SFM medium was standard at 5.5 mmol/L. Cells were sub-cultured when they reached 70–80% confluence. Twenty-four hours after reseeding, the cells were treated either with dimethyl sulfoxide or 2  $\mu$ M dapagliflozin in a serum-free culture medium for 24–48 h. As the effect of dapagliflozin was fully regulated under confluent conditions, each experiment was performed at confluence. For the D-galactose assay, HK-2 cells were incubated with the indicated concentration (0–10 mM) of D-galactose and 2  $\mu$ M dapagliflozin for 48 h.

**Animals.** Six male db/db mice (6 each, 10–12 weeks old, weighing around 50 g, male) were housed in a facility with a 12-h light/dark cycle and fed a standard chow diet (Research Diets, New Brunswick, NJ) containing 67% (Kcal) carbohydrates, 19% protein, and 4% fat *ad libitum*. All studies were approved by and performed in compliance with the guidelines of the institutional animal care and use committee of Gunma University. db/db mice were purchased from Charles River and acclimatised for 2 weeks. Dapagliflozin (0.5 mg/kg/day) dissolved with 0.5% methylcellulose was orally administered every day for 1 week. The mice were sacrificed by cerebral dislocation, and the kidneys were collected after fasting for 16 h followed by 4-h refeeding.

**Western blot analysis.** Proteins were extracted using a lysis buffer containing a protease inhibitor as described previously<sup>56</sup> and quantified using a BCA protein assay kit (Pierce, Rockford, IL, USA). Equal amounts of protein were separated using 10% sodium dodecyl sulphate–polyacrylamide gel electrophoresis and electrophoretically transferred onto nitrocellulose membranes, which were blocked with 5% fatty acid-free powdered milk for 1 h. The membranes were incubated with the following primary antibodies overnight at 4°C: anti-p-eIF2 $\alpha$  (1:500), anti-eIF2 $\alpha$  (1:1,000), anti-IRE1 (1:1,000), anti-p-IRE1 (1:1,000), anti-ATF6 (1:200), anti-ATF4 (1:500), anti-CHOP (1:500), anti-GLUT2 (1:1,000), anti-SGLT2 (1:400), and anti-tubulin- $\alpha$  (1:1,000); thereafter, they were incubated with an HRP-conjugated secondary antibody for 30 min. The membranes were extensively washed in tris-buffered saline with Tween 20, and antigen-antibody complexes were visualised by chemiluminescence using an ECL kit (Pierce).

**RNA isolation and real-time qPCR.** Total RNA was isolated from cells and tissues using the RNeasy Plus Mini Kit (Qiagen, Valencia, CA, USA) according to the manufacturer's protocol. Total RNA (1,000  $\mu$ g) was reverse-transcribed using the SuperScript VILO cDNA Synthesis Kit (Invitrogen, Carlsbad, CA, USA). Real-time quantitative PCR was performed on an Applied Biosystems 7500HT system (Applied Biosystems, Branchburg, NJ, USA) with EagleTaq Master Mix (Roche Lifescience). Gene expression levels of CHOP, ATF4, and SGLT2 were internally normalised against those of  $\beta$  actin (human) and Hrpt1 (mouse) and analysed by a standard curve method. Each experiment was performed in triplicate and independently repeated three times.

**Measurement of glucose concentration in HK2 cells.** Glucose concentration was measured using the PicoProbe Glucose Fluorometric Assay Kit (BioVision, Milpitas, CA, USA). In brief, cells were lysed and proteins were incubated with the reagents provided. Samples were transferred to black-bottom 96-well microplates, and glucose concentrations were read at excitation and emission wavelengths of 535 and 587 nm, respectively, in a fluorescence microplate reader (EnSpire, Perkin Elmer). Control reactions were carried out with no protein and/or no substrate.

**Measurement of glucose influx in HK2 cells.** Glucose influx was measured using a 2-Deoxyglucose Uptake Measurement Kit (COSMO BIO Co. Ltd., Tokyo Japan) according to the manufacturer's instructions. In brief, cells were lysed and proteins were incubated with the reagents provided. Samples were transferred to 96-well microplates, and glucose influx was read at 450 nm in a kinetic microplate reader (Molecular Devices Japan). Control reactions were carried out with no protein and/or no substrate.

**Measurement of caspase-3 activity in HK2 cells.** Caspase-3 activity was measured using a caspase-3 fluorescence assay kit (MBL) according to the manufacturer's instructions. Briefly, cells and tissues were lysed and proteins were incubated with the caspase-3 substrate DEVD-AMC (2  $\mu$ M) for 1 h at 37 °C. Samples were transferred to black-bottom 96-well microplates, and the relative caspase-3 activities were read at excitation and emission wavelengths of 380 and 460 nm, respectively, in a fluorescence microplate reader.

**Knockdown of elf2 $\alpha$  in HK2 cells.** After seeding of  $1.0\text{--}2.5 \times 10^5$  cells/12-well plates for 24 h, 100 nM siRNA for human siEIF2A-lipid complexes with DharmafectDuo (Dharmacon/Thermo Scientific, Chicago, IL) was introduced into each well. After 24 h, the medium was replaced with dimethyl sulfoxide or 2  $\mu$ M dapagliflozin and incubated for an additional 24 h. Knockdown efficiencies were confirmed by western blot analysis or real-time qPCR.

**Apoptosis and necrosis assay in HK2 cells.** An apoptosis and necrosis assay was performed using Cell Death Detection ELISApus (Roche, Indianapolis, IN) according to the manufacturer's instructions. In brief, after seeding of  $1.0 \times 10^5$  cells/96-well plates for 24 h, HK-2 cells were incubated with 7.5 ng/mL C2 ceramide and 2  $\mu$ M dapagliflozin. After 48 h, the cells were harvested to perform apoptosis and necrosis assay.

**Statistics.** The results are expressed as mean  $\pm$  standard error of the mean. Differences between cells and/or treatments were tested for statistical significance ( $P < 0.05$ ) using Student's unpaired *t* test and ANOVA multiple comparisons using Tukey's honestly significant difference test.

### Data Availability

The authors confirm that the data supporting the findings of this study are available within the article and its supplementary materials.

### References

1. Tuomilehto, J. *et al.* Prevention of type 2 diabetes mellitus by changes in lifestyle among subjects with impaired glucose tolerance. *N. Engl. J. Med.* **344**(18), 1343–1350 (2001).
2. Orozco, L. J. *et al.* Exercise or exercise and diet for preventing type 2 diabetes mellitus. *Cochrane Database Syst. Rev.* **3**, CD003054 (2008).
3. Baik, J., Nguyen, D., Nguyen, V., Hu, Z. & Abbott, G. W. Kcne2 deletion impairs insulin secretion and causes type 2 diabetes mellitus. *FASEB J.* **31**(6), 2674–2685 (2017).
4. Costantino, L., Rastelli, G., Vianello, P., Cignarella, G. & Barlocco, D. Diabetes complications and their potential prevention: aldose reductase inhibition and other approaches. *Med. Res. Rev.* **19**(1), 3–23 (1999).
5. Fan, Y., Lee, K., Wang, N. & He, J. C. The role of endoplasmic reticulum stress in diabetic nephropathy. *Curr. Diab. Rep.* **17**, 17 (2017).
6. Cunard, R. Endoplasmic reticulum stress in the diabetic kidney, the good, the bad and the ugly. *J. Clin. Med.* **4**, 715–740 (2015).
7. Cao, S. S. & Kaufman, R. J. Unfolded protein response. *Curr. Biol.* **22**(16), R622–R626 (2012).
8. Ellgaard, L., Molinari, M. & Helenius, A. Setting the standards: quality control in the secretory pathway. *Science* **286**(5446), 1882–1888 (1999).
9. Harding, H. P., Zhang, Y., Bertolotti, A., Zeng, H. & Ron, D. Perk is essential for translational regulation and cell survival during the unfolded protein response. *Mol. Cell.* **5**(5), 897–904 (2000).
10. Huber, A. L. *et al.* p58(IPK)-mediated attenuation of the proapoptotic PERK-CHOP pathway allows malignant progression upon low glucose. *Mol. Cell.* **49**(6), 1049–1059 (2013).
11. Chen, X., Shen, J. & Prywes, R. The luminal domain of ATF6 senses endoplasmic reticulum (ER) stress and causes translocation of ATF6 from the ER to the Golgi. *J. Biol. Chem.* **277**(15), 13045–13052 (2010).
12. Urano, F. *et al.* Coupling of stress in the ER to activation of JNK protein kinases by transmembrane protein kinase IRE1. *Science* **287**(5453), 664–666 (2000).
13. Liu, G. *et al.* Apoptosis induced by endoplasmic reticulum stress involved in diabetic kidney disease. *Biochem. Biophys. Res. Commun.* **370**(4), 651–656 (2008).
14. Basha, B., Samuel, S. M., Triggie, C. R. & Ding, H. Endothelial dysfunction in diabetes mellitus: possible involvement of endoplasmic reticulum stress? *Exp. Diabetes Res.* **2012**, 481840 (2012).
15. Zhong, Y. *et al.* Activation of endoplasmic reticulum stress by hyperglycemia is essential for Müller cell-derived inflammatory cytokine production in diabetes. *Diabetes* **61**(2), 492–504 (2012).
16. Ponnusamy, S. *et al.* Sphingolipids and cancer: ceramide and sphingosine-1-phosphate in the regulation of cell death and drug resistance. *Future Oncol.* **6**(10), 1603–1624 (2010).
17. Movsesyan, V. A., Yakovlev, A. G., Dabaghyan, E. A., Stoica, B. A. & Faden, A. I. Ceramide induces neuronal apoptosis through the caspase-9/caspase-3 pathway. *Biochem. Biophys. Res. Commun.* **299**(2), 201–207 (2002).
18. Haus, J. M. *et al.* Plasma ceramides are elevated in obese subjects with type 2 diabetes and correlate with the severity of insulin resistance. *Diabetes* **58**(2), 337–343 (2009).
19. Yaribeygi, H., Bo, S., Ruscica, M. & Sahebkar, A. Ceramides and diabetes mellitus: an update on the potential molecular relationships. *Diabet Med.* **Feb 25** (2019).
20. Galadari, S. *et al.* Role of ceramide in diabetes mellitus: evidence and mechanisms. *Lipids in Health and Disease* **12**(98) (2013).
21. Srivastava, S. P. *et al.* Lipid mediators in diabetic nephropathy. *Fibrogenesis Tissue Repair.* **7–12** (2014).
22. Choi, S. R. *et al.* Adiponectin receptor agonist AdipoRon decreased ceramide, and lipotoxicity, and ameliorated diabetic nephropathy. *Metabolism.* **85**, 348–360 (2018).
23. Bonventre, J. V. Can we target tubular damage to prevent renal function decline in diabetes? *Semin. Nephrol.* **32**(5), 452–462 (2012).
24. Mosley, J. F. II, Smith, L., Everton, E. & Fellner, C. Sodium-glucose linked transporter 2 (SGLT2) inhibitors in the management of type-2 diabetes: a drug class overview. *P T.* **40**(7), 451–462 (2015).
25. Gnudi, L., Coward, R. J. & Long, D. A. Diabetic nephropathy: perspective on novel molecular mechanisms. *Trends Endocrinol. Metab.* **27**(11), 820–830 (2016).
26. Zhang, J., Fan, Y., Zeng, C., He, L. & Wang, N. Tauroursodeoxycholic acid attenuates renal tubular injury in a mouse model of type 2 diabetes. *Nutrients* **8**(10) (2016).
27. Cao, A. L. *et al.* Ursodeoxycholic acid and 4-phenylbutyrate prevent endoplasmic reticulum stress-induced podocyte apoptosis in diabetic nephropathy. *Lab. Invest.* **96**(6), 610–622 (2016).
28. Fan, Y. *et al.* Rtn1a-Mediated Endoplasmic Reticulum Stress in Podocyte Injury and Diabetic Nephropathy. *Sci Rep.* **7**(1), 323 (2017).
29. Chen, J. *et al.* stress triggers MCP-1 expression through SET7/9-induced histone methylation in the kidneys of db/db mice. *Am J Physiol Renal Physiol.* **306**(8), F916–925 (2014).

30. Jia, Y. *et al.* Dapagliflozin Aggravates Renal Injury via Promoting Gluconeogenesis in db/db Mice. *Cellular Physiology and Biochemistry* **45**, 1747–1758 (2018).
31. Terami, N. *et al.* Long-term treatment with the sodium glucose cotransporter 2 inhibitor, dapagliflozin, ameliorates glucose homeostasis and diabetic nephropathy in db/db mice. *PLoS One* **9**(6) (2014).
32. Bakris, G. L., Fonseca, V. A., Sharma, K. & Wright, E. M. Renal sodium-glucose transport: role in diabetes mellitus and potential clinical implications. *Kidney Int.* **75**(12), 1272–1277 (2009).
33. Komoroski, B. *et al.* Dapagliflozin, a Novel SGLT2 Inhibitor, Induces Dose-Dependent Glucosuria in Healthy Subjects. *Clinical Pharmacology & Therapeutics* (2009)
34. Kasichayanula, S. *et al.* Clinical Pharmacokinetics and Pharmacodynamics of Dapagliflozin, a Selective Inhibitor of Sodium-Glucose Co-transporter Type 2. *Clinical Pharmacokinetics* **53**(1), 17–27 (2014).
35. Lim, J. C. *et al.* Cannabinoid receptor 1 mediates high glucose-induced apoptosis via endoplasmic reticulum stress in primary cultured rat mesangial cells. *American Journal of Physiology-Renal Physiology* **301**(1) (2011).
36. Chang, Y. K. *et al.* Dapagliflozin, SGLT2 Inhibitor, Attenuates Renal Ischemia-Reperfusion Injury. *PLoS One.* **8**, **11**(7) (2016).
37. Lu, Y. T. *et al.* A Fluorescent Glucose Transport Assay for Screening SGLT2 Inhibitors in Endogenous SGLT2-Expressing HK-2 Cells. *Nat Prod Bioprospect.* **9**(1), 13–21 (2019).
38. Kothinti, R. K., Blodgett, A. B., North, P. E., Roman, R. J. & Tabatabai, N. M. A novel SGLT is expressed in the human kidney. *Eur J Pharmacol.* **5**;690(1–3), 77–83 (2012).
39. Karunakaran, U. *et al.* Myricetin Protects Against High Glucose-Induced  $\beta$ -Cell Apoptosis by Attenuating Endoplasmic Reticulum Stress via Inactivation of Cyclin-Dependent Kinase 5. *Diabetes Metab J.* **43**(2), 192–205 (2019).
40. Ma, L. *et al.* Low glucose and metformin-induced apoptosis of human ovarian cancer cells is connected to ASK1 via mitochondrial and endoplasmic reticulum stress-associated pathways. *J Exp Clin Cancer Res* **38**(1), 77 (2019).
41. Chang, J. W. *et al.* Up-Regulation of SIRT1 Reduces Endoplasmic Reticulum Stress and Renal Fibrosis. *Nephron.* **133**(2), 116–128 (2016).
42. Jiang, X. *et al.* Overexpression of augments of liver regeneration (ALR) mitigates the effect of H<sub>2</sub>O<sub>2</sub>-induced endoplasmic reticulum stress in renal tubule epithelial cells. *Apoptosis.* **24**(3–4), 278–289 (2019).
43. Lin, M. *et al.* Baicalin ameliorates H<sub>2</sub>O<sub>2</sub> induced cytotoxicity in HK-2 cells through the inhibition of ER stress and the activation of Nrf2 signaling. *Int J Mol Sci.* **15**;15(7), 12507–12522 (2014).
44. Zhou, X. *et al.* Propofol decreases endoplasmic reticulum stress-mediated apoptosis in retinal pigment epithelial cells. *PLoS One* **11**(6), e0157590 (2016).
45. Ozcan, L. & Tabas, I. Role of endoplasmic reticulum stress in metabolic disease and other disorders. *Annu. Rev. Med.* **63**, 317–328 (2012).
46. Zhang, K. & Kaufman, R. J. From endoplasmic-reticulum stress to the inflammatory response. *Nature* **454**(7203), 455–462 (2008).
47. Wu, X., He, Y., Jing, Y., Li, K. & Zhang, J. Albumin overload induces apoptosis in renal tubular epithelial cells through a CHOP-dependent pathway. *OMICS* **14**(1), 61–73 (2010).
48. Wang, M. & Kaufman, R. J. The impact of the endoplasmic reticulum protein-folding environment on cancer development. *Nat. Rev. Cancer* **14**(9), 581–597 (2014).
49. Ogretmen, B. & Hannun, Y. A. Biologically active sphingolipids in cancer pathogenesis and treatment. *Nat. Rev. Cancer* **4**(8), 604–616 (2004).
50. Ueda, N., Kaushal, G. P., Hong, X. & Shah, S. V. Role of enhanced ceramide generation in DNA damage and cell death in chemical hypoxic injury to LLC-PK1 cells. *Kidney Int.* **54**(2), 399–406 (1998).
51. Basnakian, A. G. *et al.* Ceramide synthase is essential for endonuclease-mediated death of renal tubular epithelial cells induced by hypoxia-reoxygenation. *Am. J. Physiol. Renal Physiol.* **288**(2), F308–F314 (2005).
52. Komoroski, B. *et al.* Dapagliflozin, a novel, selective SGLT2 inhibitor, improved glycemic control over 2 weeks in patients with type 2 diabetes mellitus. *Clin. Pharmacol. Ther.* **85**(5), 513–519 (2009).
53. Wanner, C. *et al.* EMPA-REG OUTCOME Investigators. Empagliflozin and Progression of Kidney Disease in Type 2 Diabetes. *N Engl J Med.* Jul **28**;375(4), 323–34 (2016).
54. Neal, B. *et al.* CANVAS Program Collaborative Group. Canagliflozin and Cardiovascular and Renal Events in Type 2 Diabetes. *N Engl J Med.* Aug **17**;377(7), 644–657(2017).
55. Zinman, B. *et al.* Empagliflozin, cardiovascular outcomes, and mortality in type 2 diabetes. *N. Engl. J. Med.* **373**(22), 2117–2128 (2015).
56. Yamada, E. *et al.* Fyn phosphorylates AMPK to inhibit AMPK activity and AMP-dependent activation of autophagy. *Oncotarget* **7**(46), 74612–74629 (2016).

## Author Contributions

Conceived, designed/performed the experiments, analysed the data, and wrote the paper: E.Y. Performed the experiments, analysed the data, and wrote the paper: R.S. Analysed the data and wrote the paper: C.B. Analysed the data: S.O., Y.N., A.M., K.K. and M.Y.

## Additional Information

**Supplementary information** accompanies this paper at <https://doi.org/10.1038/s41598-019-46402-6>.

**Competing Interests:** The authors declare no competing interests.

**Publisher's note:** Springer Nature remains neutral with regard to jurisdictional claims in published maps and institutional affiliations.



**Open Access** This article is licensed under a Creative Commons Attribution 4.0 International License, which permits use, sharing, adaptation, distribution and reproduction in any medium or format, as long as you give appropriate credit to the original author(s) and the source, provide a link to the Creative Commons license, and indicate if changes were made. The images or other third party material in this article are included in the article's Creative Commons license, unless indicated otherwise in a credit line to the material. If material is not included in the article's Creative Commons license and your intended use is not permitted by statutory regulation or exceeds the permitted use, you will need to obtain permission directly from the copyright holder. To view a copy of this license, visit <http://creativecommons.org/licenses/by/4.0/>.

© The Author(s) 2019